53. Molecular Electronics

The prospects of using organic materials in electronics and optoelectronics applications have attracted scientists and technologists since the 1970s. This field has become known as **molecular electronics**. Some successes have already been achieved, for example the liquid-crystal display. Other products such as organic light-emitting displays, chemical sensors and plastic transistors are developing fast. There is also a keen interest in exploiting technologies at the molecular scale that might eventually replace silicon devices. This chapter provides some of the background physics and chemistry to the interdisciplinary subject of molecular electronics. A review of some of the possible application areas for organic materials is presented and some speculation is provided regarding future directions.

Molecular electronics is concerned with the exploitation of organic and biological materials in electronics and optoelectronics [53.1–3]. The subject, as it has matured over the last 30 years, can broadly be divided into two themes. The first area, *molecular materials for electronics*, has its origins in materials science and concerns the development of devices that utilise the unique macroscopic properties of organic compounds. The most successful commercial product to date is the liquid-crystal display. However, following many years of research, devices such as organic light-emitting displays, pyroelectric detectors for infrared imaging, and chemical and biochemical sensors are beginning to make a technological impact. The Nobel prize in Chemistry for 2000 was awarded to three scientists working in this area: Alan Heeger, Alan MacDiarmid and Hideki Shirakawa, who have made significant contributions to the development of electrically conductive polymers. More challenging is *molecular-scale electronics*. Here, the focus is on the behaviour of individual organic molecules or groups of molecules. Topics such as molecular switches [53.3–9], molecular memories [53.10–13], molecular rectifiers [53.14], negative differential-resistance junctions [53.15], deoxyribonucleic acid (DNA) electronics [53.16] and molecular manufacturing [53.17,18] have all been described in the literature. It is much too early to say which, if any, of these could find their way into the commercial arena.

This chapter provides an introduction to the interdisciplinary world of molecular electronics. In the first instance, the physics background to semiconductive organic compounds is outlined. A review of the available materials is presented and some of the possible device applications are described. There are currently a limited number of ways in which organic molecules can be deposited and manipulated on surfaces to form solid films, which can then be used in device structures. The most popular methods are outlined, and methods to pattern the films are described. The prospects for molecular-scale electronics are contrasted with the progress of the inorganic semiconductor industry. Finally, a selection of the ongoing work on molecular-scale devices is described and some speculation about future developments is given.

53.1 Electrically Conductive Organic Compounds

Metallic and semiconductive behaviour is not restricted to inorganic materials. Figure 53.1 shows that the room-temperature conductivity values for organic polymers can extend over much of the spectrum of electrical conductivity, from insulating to semiconducting, and even metallic, behavior [53.19]. The physical explanation can be found in the nature of the chemical bonds that hold solids together.

53.1.1 Orbitals and Chemical Bonding

Carbon-based materials are unique in many respects. This is due to the many possible configurations of the electronic states of a carbon atom. Carbon has an atomic number of six and a valency of four. Its electron configuration is $1s^2$, $2s^2$, $2p^2$, i. e. the inner 1s shell is filled and the four valence electrons available for bonding are distributed two in the 2s orbital and two in the 2p orbitals. As the 2s orbital is spherically symmetrical, Fig. 53.2, it can form a bond in any direction. In contrast, the 2p orbitals are directed along mutually orthogonal axes and will tend to form bonds in these directions. When two or more of the valence electrons of carbon are involved in bonding with other atoms, the bonding can be explained by the construction of *hybrid* orbitals by mathematically combining the 2s and 2p orbitals. In the simplest case, the carbon 2s orbital hybridises with a single p orbital. Taking the sum and difference of the two orbitals gives two sp *hybrids*; two p orbitals then remain. The sp orbitals are constructed from equal amounts of s and p orbitals; they are linear and 180° apart.

Other combinations of orbitals lead to different hybrids. For example, from the 2s orbital and two 2p orbitals (e.g. a $2p_x$ and a $2p_y$), three equivalent sp^2 hybrids may be constructed. Each orbital is 33.3% s and 66.7% p. The three hybrids lie in the xy plane (the same plane defined by the two p orbitals), directed 120° from each other, and the remaining p orbital is perpendicular to the sp^2 plane. Four sp^3 hybrids may be derived from an s orbital and three p orbitals. These are directed to the corners of a tetrahedron with an angle between the bonds of 109.5°; each orbital is 25% s and 75% p.

A chemical bond can also be formed from a mixture of the above hybrid orbitals, e.g. it is possible to have a hybridised orbital that is 23% s and 77% p. Thus, sp, sp^2 and sp^3 hybrids must be considered as limiting cases. Electrons in s orbitals have a lower energy than electrons in p orbitals. Therefore, bonds with more s character tend to be stronger.

Carbon forms four bonds in most compounds, resulting from its four valence electrons. In ethane, C_2H_6, the C−H bonds are all approximately $C(sp^3)$−H(s) while the C−C bond is approximately $C(sp^3)$−$C(sp^3)$. However, in the ethylene molecule, C_2H_4, each of the two carbons is attached to just three atoms while in acetylene, C_2H_2, each carbon atom is only attached to one carbon. In these compounds, the two carbon atoms are bound together by double (CH_2=CH_2) or triple (CH≡CH) bonds, which involve sp^2 and sp hybrids, respectively. These bonds can be considered to have two distinct components. For example, in ethylene, two sp^2 hybrids on each carbon bond with the hydrogens. A third sp^2 hy-

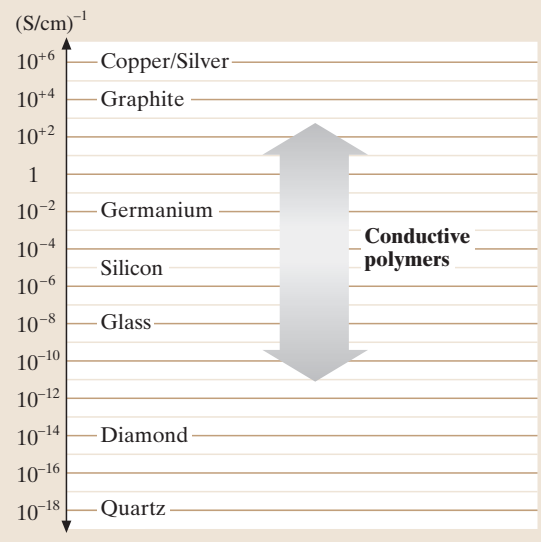

Fig. 53.1 Room-temperature conductivity values of conductive polymers compared to other materials. (After *Roth* [53.19], with permission © Wiley)

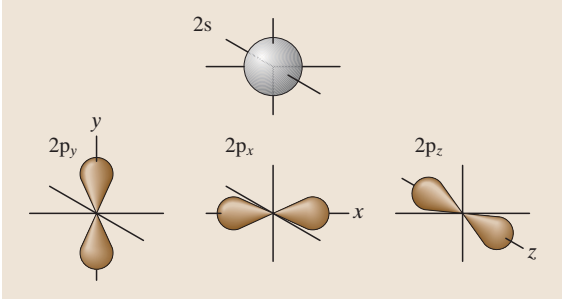

Fig. 53.2 *Top*: 2s orbital. *Bottom*: $2p_y$, $2p_x$ and $2p_z$ orbitals

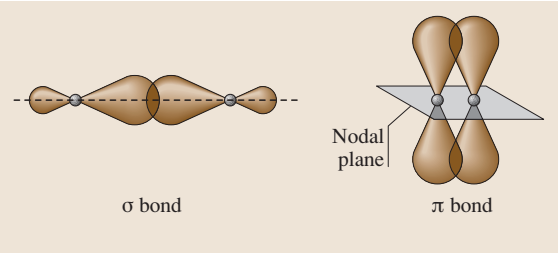

Fig. 53.3 Sigma (σ) and pi (π) bonding

brid on each carbon forms a $C(sp^2)-C(sp^2)$ single bond, leaving a p orbital 'left-over' on each carbon. This orbital lies perpendicular to the plane of the six atoms. The two p orbitals are parallel to each other and have regions of overlap above and below the molecular plane. This type of bond, consisting of two separate sausage-like electron clouds lying above and below the planes of the carbon nuclei, is called a pi (π) bond. In contrast, the bond formed by the head-on overlap of the two carbon sp^2 orbitals is known as a sigma (σ) bond and the electron cloud is densest at the midpoint between the carbon nuclei. The π bond has little electron density in the region between the carbon atoms and is much weaker than the σ bond. Figure 53.3 illustrates sigma and pi bonding. Carbon compounds that contain π bonds are said to be unsaturated, meaning that the carbon atoms, while having formed the requisite number of bonds, are not fully saturated in terms of their number of potential neighbours. Saturated carbon molecules, on the other hand, contain only single bonds.

53.1.2 Band Theory

The application of quantum mechanics to the electrons in the bonds of inorganic semiconductors led to the development of band theory, one of the great success stories of modern physics. Whenever two identical atoms are brought close together, the electron orbitals overlap and the energy level associated with each electron in the separated atoms is split into two new levels, with one above and one below the original level. A rigorous, quantum-mechanical description of the bonding reveals that the total number of orbitals must be conserved, i. e. the total number of molecular orbitals must be the same as the number of atomic orbitals that went into their formation. Consider, for example, the formation of a hydrogen molecule from two separated atoms. When the two atoms approach each other so that their 1s orbitals overlap, two new orbitals (σ bonds) are formed around the atoms, symmetric with respect to the interatomic axis. In one orbital, the bonding orbital, the electron has a lower energy than in the isolated atomic orbital and in the other, the antibonding orbital, an electron has a higher energy. In the hydrogen molecule, the electron pair normally resides in the bonding orbital. The energy of the electrons in this orbital is lowered relative to that in the atomic orbitals, which is why the atoms remain bound together.

In an extended solid many atoms can interact and many similar splittings of energy levels occur. For a solid containing approximately 10^{26} atoms (Avogadro's number) each energy level splits, but the energies between these split levels are very small and continuous ranges or bands of energy are formed. Two such important bands are the valence band and the conduction band, analogous to the bonding and antibonding levels of the two-atom model. The energy gap, or band gap, between them is a forbidden energy range for electrons. Electrical conduction takes place by electrons moving under the influence of an applied electric field in the conduction band and/or holes moving in the valence band. Holes are really vacancies in a band but, for convenience, they may be regarded as positively charged carriers. For an electron, or hole, to gain energy from an applied electric field, and therefore for conductivity to occur, the charge carrier must be able to move into an unoccupied higher energy state. If the carrier cannot be accelerated by the field, then it cannot contribute to the electrical conduction. In a metal, the various energy bands overlap to provide a single energy band that is only partly full of electrons. An insulator has a full valence band and a relatively large energy separation (> 5 eV) to the higher conduction band. Most semiconductors possess the band structure of an insulator, but a forbidden energy gap of only 0.1–3 eV, so that carriers may be produced in the conduction and/or valence bands by optical or thermal means, or by doping with impurities.

An important feature of the band model is that the electrons are delocalised or spread over the lattice. The strength of the interaction between the overlapping orbitals determines the extent of delocalisation that is possible for a given system. For many polymeric organic materials, the molecular orbitals responsible for bonding the carbon atoms of the chain together are the sp^3 hybridised σ bonds, which do not give rise to extensive overlapping. The resulting band gap is large, as the electrons involved in the bonding are strongly localised on the carbon atoms and cannot contribute to the conduction process. This is why a simple saturated polymer such as polyethylene, $(CH_2)_n$, is an electrical insulator.

A significant increase in the degree of electron delocalisation may be found in unsaturated polymers, i. e.

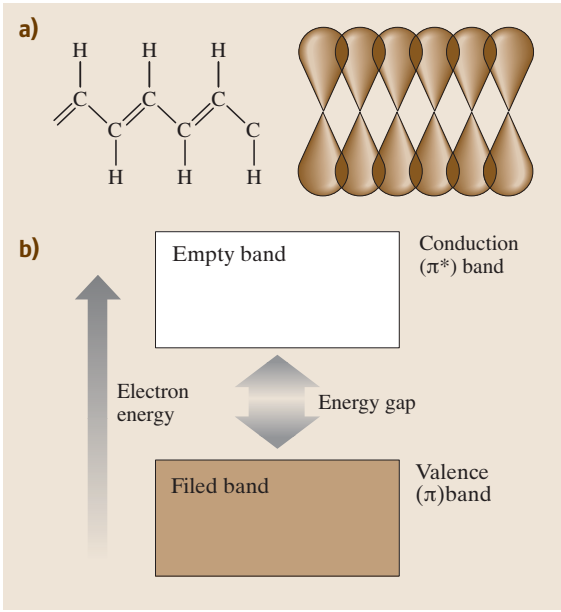

Fig. 53.4 (a) Chemical π bonding in polyacetylene. **(b)** Electronic band structure showing the normally empty π^* band (conduction band) and the normally filled π band (valence band)

those containing double and triple carbon–carbon bonds. If each carbon atom along the chain has only one other atom, e.g. hydrogen, attached to it, the spare electron in a p_z-orbital of the carbon atom overlaps with those of carbon atoms on either side forming delocalised molecular orbitals of π-symmetry. For a simple lattice of length $L = Na$, where N is the total number of atoms and a is the spacing between them, it can be shown that the total number of electron states in the lowest energy band is equal to N. This result is true for every energy band in the system and applies to three-dimensional lattices. Allowing for the two spin orientations of an electron, the Pauli exclusion principle requires that there will be room for two electrons per cell of the lattice in an energy band. If each atom contributes one bonding electron, the valence band will be only half filled.

It might therefore be expected that a linear polymer backbone consisting of many strongly interacting coplanar p_z orbitals, each of which contributes one electron to the resultant continuous π electron system, would behave as a one-dimensional metal with a half-filled band. In chemical terms, this is a conjugated chain and may be represented by a system of alternating single and double bonds. It turns out that, for one-dimensional systems, such a chain can more efficiently lower its energy by introducing bond alternation (alternating short and long bonds). This limits the extent of electronic delocalisation that can take place along the backbone. The effect is to open an energy gap in the electronic structure of the polymer. All conjugated polymers are semiconductors, with band gaps more than about 1.5 eV, rather than metals (N.B. the band gap in silicon is 1.1 eV at room temperature). Figure 53.4 shows the chemical π bonding and the electronic band structure of polyacetylene.

53.1.3 Electrical Conductivity

In polyacetylene, the valence band, or π band, is normally filled with electrons while the conduction band, or π^* band is normally empty. Like silicon, the conductivity of polyacetylene can be changed by the addition of impurity atoms. However, the term *doping* is a misnomer as it tends to imply the use of minute quantities, parts per million or less, of impurities introduced into a crystal lattice. In the case of conductive polymers, typically 1% to 50% by weight of chemically oxidising (electron withdrawing) or reducing (electron donating) agents are used to alter physically the number of π-electrons on the polymer backbone, leaving oppositely charged counterions alongside the polymer chain. These processes are redox chemistry. For example, the halogen doping process that transforms polyacetylene to a good conductor is oxidation (or p-doping).

$$[\mathrm{CH}]_n + \frac{3x}{2}\mathrm{I}_2 \rightarrow [\mathrm{CH}]_n^{x+} + x\mathrm{I}_3^- \,.$$

Reductive doping (n-doping) is also possible, e.g. using an alkali metal.

$$[\mathrm{CH}]_n + x\mathrm{Na} \rightarrow [\mathrm{CH}]_n^{x-} + x\mathrm{Na}^+ \,.$$

In both cases, the doped polymer is a salt. The counterions, I_3^- or Na^+, are fixed in position while the charges on the polymer backbone are mobile and contribute to the conductivity. The doping effect can be achieved because a π electron can be removed (or added) without destroying the σ backbone of the polymer so that the charged polymer remains intact. The increase in conductivity can be as much as eleven orders of magnitude.

The electrical properties of semiconductive organic polymers are not directly comparable to those of silicon. An important material parameter is the mobility of the charge carriers μ. This determines the (additional) velocity that a charge carrier (an electron or hole) acquires because of an applied electric field, and is defined by

$$\mu = \frac{v_\mathrm{d}}{E} \,,$$

Table 53.1 Room-temperature field-effect carrier mobilities for field-effect transistors based on organic semiconductors [53.20,21]. The electron mobilities in single-crystal silicon and gallium arsenide are also given

Material	Mobility (cm^2/Vs)
Si single crystal (electrons)	1500
GaAs single crystal (electrons)	8500
Polythiophene	10^{-5}
Polyacetylene	10^{-4}
Phthalocyanine	10^{-4}–10^{-2}
Thiophene oligomers	10^{-4}–10^{-1}
Organometallic dmit complex	0.2
Pentacene	10^{-3}–1
C_{60}	0.3

where v_d is the drift velocity of the carrier and E is the electric field. The mobility may be further related to the electrical conductivity σ by the expression

$$\sigma = |q|\, n\mu\,,$$

where n is the density of charge carriers and $|q|$ is the magnitude of their charge (charge on an electron $= 1.6\times10^{-19}$ C). The carrier mobility provides an indication of how quickly the carriers react to the field (i. e. the frequency response of the material). The greater the degree of electron delocalisation, the larger the width of the bands (in energy terms) and the higher the mobility of the carriers within the band. For inorganic semiconductors such as silicon or gallium arsenide, the three-dimensional crystallographic structure provides for extensive carrier delocalisation throughout the solid, resulting in a relatively high mobility μ.

Electrical conduction in polymers not only requires carrier transport along the polymer chains but some kind or transfer, or *hopping*, between these chains, which tend to lie tangled up like a plate of spaghetti. The charge-carrier mobilities in organic polymers are therefore quite low, making it difficult to produce very high-speed electronic computational devices that are competitive with those based on silicon and gallium arsenide. However, some improvement in the carrier mobility can be achieved by both increasing the degree of order of the polymer chains and by improving the purity of the material. Table 53.1 contrasts the room-temperature carrier mobility values for Si, GaAs and a number of different conductive organic compounds [53.20, 21]. Although the values are quite low for the organic materials, other features make them attractive for certain types of electronic device, as indicated in the later sections.

53.2 Materials

Many conductive polymers have been synthesised to provide certain electronic features (e.g. band gap, electron affinity). The monomer repeat units are often based on five- or six-membered (benzene) carbon ring systems, including polypyrrole, polythiophene (and various other polythiophene derivatives), polyphenelenevinylene and polyaniline [53.22]. The chemical structure of some of these materials is shown in Fig. 53.5. Such polymers generally show lower electrical conductivity than polyacetylene, however they can have the advantage of high stability and processability.

Conductive polymers represent only one category of organic electrical conductors. Another important class are the charge-transfer compounds [53.23, 24]. These are formed from a variety of molecules, primarily aromatic compounds (i. e. based on benzene) which can behave as electron donors (d) and electron acceptors (a). Complete transfer of an electron from a donor to an acceptor molecule results in a system that is electrically insulating (e.g. the transfer of a valence electron in a Na atom to a Cl atom, forming the compound NaCl). However, if the ratio of the number of donor molecules to the number of acceptor molecules differs from 1 : 1, e.g. the stoichiometry is 1 : 2 or 2 : 3, or if there is incomplete transfer of an electron from a donor to an acceptor (say,

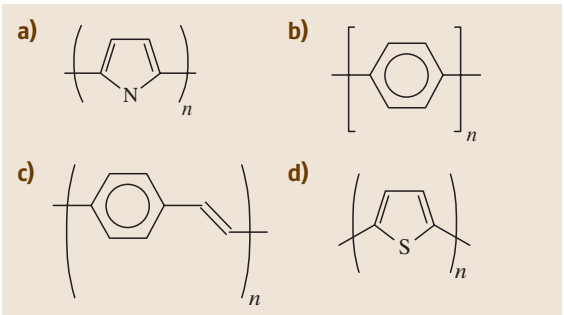

Fig. 53.5a–d Chemical structures of conductive polymers: **(a)** polypyrrole, **(b)** polyparaphenylene, **(c)** polyphenylene-vinylene, and **(d)** polythiophene

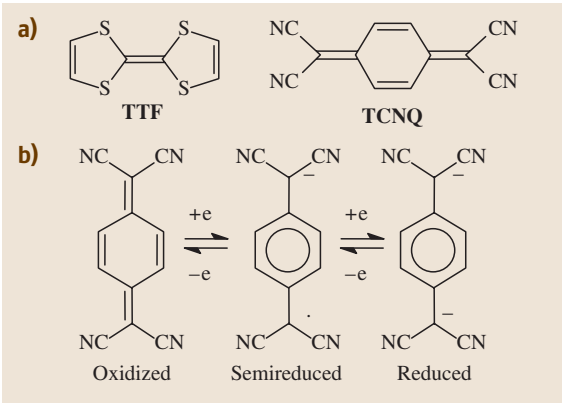

Fig. 53.6 **(a)** Chemical structures of the charge-transfer compounds tetrathiafulvalene (TTF) and tetracyanoquinodimethane (TCNQ). **(b)** Oxidation and reduction of TCNQ

six electrons in every ten are transferred), then partially filled electron energy bands can be formed and electron conduction is possible.

Charge-transfer interactions are strongest between donor molecules of low ionisation potential and acceptor molecules of high electron affinity, provided that the donor and acceptor molecules have similar symmetry and are able to approach closely [53.24]. Well-known donor and acceptor molecules are tetrathiafulvalene (TTF) and tetracyanoquinodimethane (TCNQ), Fig. 53.6a. The latter compound is a very strong acceptor forming first the radical anion and then the dianion, Fig. 53.6b. The stability of the semireduced radical ion, $TCNQ^{-\bullet}$, with respect to the neutral molecule mainly arises from the change from the relatively unstable quinoid structure to the aromatic one, allowing extensive delocalisation of the π electrons over the carbon skeleton. As a consequence, TCNQ not only forms typical charge-transfer complexes but is also able to form true radical-ion salts, incurring complete one-electron transfer. Thus, on addition of lithium iodide to a solution of TCNQ, the simple lithium TCNQ salt is formed:

$$TCNQ + LiI \Leftrightarrow Li^{+}TCNQ^{-\bullet} + \frac{1}{2}I_2 \,.$$

Following removal of the free iodine precipitate, the TCNQ salt may be crystallised. The crystals show an electronic conductivity of about 10^{-5} S/cm.

A 1 : 1 TCNQ : TTF salt exhibits a high room-temperature conductivity (5×10^2 S/cm) and metallic behaviour is observed as the temperature is reduced to 54 K. The molecules in such compounds are arranged in segregated stacks, in which the donors and acceptors form separate donor stacks (ddddd...) and acceptor stacks (aaaaa...). The molecules are stacked in such a way that the π bonds on successive molecules can overlap to form bands. This overlap is different from the p-orbital overlap forming the π bands in conjugated polymers. The crystalline packing in these, and other, charge-transfer compounds generally leads to carrier mobility values that are higher than for semiconductive polymers.

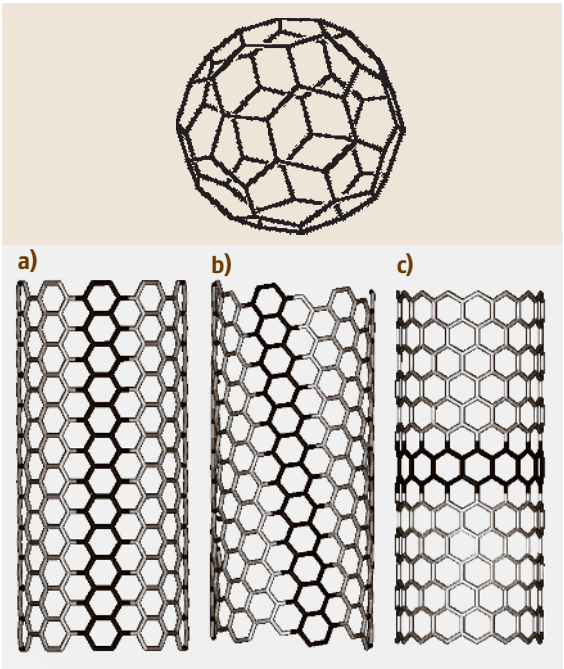

Fig. 53.7a–c Chemical structure of C_{60} (*top*) and three classes of single-wall carbon nanotube (SWNT) **(a)** (10,10) armchair SWNT, **(b)** (12,7) chiral SWNT and **(c)** (15,0) zigzag SWNT

Other electroactive compounds that may find application in molecular electronics are based on forms of pure carbon. Graphite consists of vast carbon sheets stacked one on top of another like a sheaf of papers. In pure graphite, these layers are about 0.335 nm apart, but they can be separated further by intercalating various molecules. The bonding between the carbon atoms in the planes is mainly sp^2 hybridisations consisting of a network of single and double bonds. Weak interactions between the delocalised electron orbitals hold adjacent sheets together. The delocalised electron system in the planes results in semiconductive electrical behaviour.

Under certain conditions, carbon forms regular clusters of 60, 70, 84 etc. atoms [53.25, 26]. A C_{60} cluster,

shown in Fig. 53.7, is composed of 20 hexagons and 12 pentagons and resembles a football. The diameter of the ball is about 1 nm. As with graphite, each carbon atom in C_{60} is bonded to three other carbon atoms. Thus C_{60} can be considered as a rolled up layer of a single graphite sheet. The term buckminsterfullerene was given originally to the C_{60} molecule because of the resemblance to the geodesic domes designed and built by Richard Buckminster Fuller. However, this term (or fullerene or buckyball) is used quite generally to describe C_{60} and related compounds. For example, a molecule with the formula C_{70} can be formed by inserting an extra ring of hexagons around the equator of the sphere, producing an elongated shell more like a rugby ball.

In addition to the spherical-shaped fullerenes, it is possible to synthesise tubular variations – carbon nanotubes [53.26, 27]. Such tubes are comprised of graphite-like sheets curled into a cylinder. Each tube may contain several cylinders nested inside each other. The tubes are capped at the end by cones or faceted hemispheres. Because of their very small diameters (down to around 0.7 nm), carbon nanotubes are prototype one-dimensional nanostructures. An important feature of a carbon nanotube is the orientation of the six-membered carbon ring in the honeycomb lattice relative to the axis of the nanotube. Three examples of single-wall carbon nanotubes (SWCNs) are shown in Fig. 53.7. The primary classification of a carbon nanotube is as either being chiral or achiral. An achiral nanotube is one whose mirror image has an identical structure to the original. There are only two cases of achiral nanotubes: armchair and zigzag (these names arise from the shape of the cross-sectional ring). Chiral nanotubes exhibit a spiral symmetry whose mirror image cannot be superimposed on the original structure. Carbon nanotubes are characterised by the chiral index (n, m) where the integers n and m specify each carbon nanotube uniquely [53.27]. An armchair nanotube corresponds to the special case $n = m$, while for a zigzag nanotube $m = 0$. All other (n, m) indexes correspond to chiral nanotubes. The electronic structure of a SWCN is either metallic or semiconducting, depending on its diameter and chirality.

At low temperature, a single-wall carbon nanotube is a quantum wire in which the electrons in the wire move without being scattered. Resistance measurements for various nanotube samples show that there are metallic and semiconducting nanotubes [53.27]. Carbon nanotubes can also be doped either by electron donors or electron acceptors [53.28]. After reaction with the host materials, the dopants are intercalated in the intershell spaces of the multiwalled nanotubes, and, in the case of single-walled nanotubes, either in between the individual tubes or inside the tubes.

The above confirms carbon's uniqueness as an electronic material. It can be a good conductor in the form of graphite, an insulator in the form of diamond, or a flexible polymer (conductive or insulating) when reacted with hydrogen and other species. Carbon differs from other group IV elements, such as Si and Ge, which exhibit sp^3 hybridisation. Carbon does not have any inner atomic orbitals except for the spherical 1s orbital, and the absence of nearby inner orbitals facilitates hybridisations involving only the valence (outer) s and p orbitals. The fact that sp and sp^2 hybridisations do not readily occur in Si and Ge might be related to the absence of *organic materials* made from these elements.

53.3 Plastic Electronics

53.3.1 Diodes and Transistors

Since the discovery of semiconducting behaviour in organic materials, there has been a considerable research effort aimed at exploiting these properties in electronic and optoelectronic devices. The term *plastic electronics* refers to electronic devices incorporating polymeric organic compounds (although this term is often used more widely to include devices incorporating other semiconducting organic materials). Organic semiconductors can have significant advantages over their inorganic counterparts. For example, thin layers of polymers can easily be made by low-cost methods such as spin coating. High-temperature deposition from vapour reactants is generally needed for inorganic semiconductors. Synthetic organic chemistry also offers the possibility of designing new materials with different band gaps. As noted in Sect. 53.1.3, the mobilities of the charge carriers in organic field-effect transistors are low. Nevertheless, the simple fabrication techniques for polymers have attracted several companies to work on polymer transistor applications such as data storage and thin-film device arrays to address liquid-crystal displays [53.20, 29–31].

Semiconducting organic compounds have been used in a similar fashion to inorganic semiconductors (e.g. Si, GaAs) in metal/semiconductor/metal structures. A diode, or rectifying device, can be made by sandwiching a semiconductor between metals of different work functions. In the ideal case, an n-type semiconductor should make an Ohmic contact to a low-work-function metal and a rectifying Schottky barrier to a high-work-function metal [53.32]. One example is that of a semiconductive organic film sandwiched between aluminium and indium-tin-oxide electrodes [53.33]. This device also exhibits photovoltaic behaviour.

Organic materials have been used as the semiconducting layer in field-effect transistor (FET) devices [53.20, 34–36]. These are three-terminal structures: a voltage applied to a metallic gate affects an electric current flowing between the source and drain electrodes. For transistor operation, charge must be injected easily from the source electrode into the organic semiconductor and the carrier mobility should be high enough to allow useful quantities of source–drain current to flow. The organic semiconductor and other materials with which it is in contact must also withstand the operating conditions without thermal, electrochemical or photochemical degradation. Two performance parameters to be optimised in organic field-effect transistors are the field-effect mobility and the on/off ratio [53.35].

The operating characteristics of organic transistors and integrated circuits have improved markedly over recent years. This has been brought about by both improvements in the material synthesis and in the thin-film processing techniques [53.37–45]. State-of-the-art organic FETs possess characteristics similar to those of devices prepared from hydrogenated amorphous silicon, with mobilities around 1 cm^2/Vs and on/off ratios greater than 10^6. A number of groups have also demonstrated transistor devices incorporating carbon nanotubes [53.46–48]. However, some key issues need to be addressed before nanotubes can be exploited fully in such applications. These include the reproducible fabrication of low-resistance electrical contacts and the accurate control of nanotube growth parameters [53.49]. The nanotube transistor devices realised experimentally have typical dimensions in the micron range. The real promise of carbon nanotube devices, however, lies in the possibility of nanoscale devices.

Thin-film transistors based on organic semiconductors are likely to form key components of plastic circuitry for use as display drivers in portable computers and pagers, and as memory elements in transaction cards and identification tags.

53.3.2 Organic Light-Emitting Structures

Reports of light emission from organic materials on the application of an electric field (electroluminescence) have been around for many years. However, there has been an upsurge in interest following the initial report of organic light-emitting devices (OLEDs) incorporating the conjugated polymer polyphenylenevinylene (PPV, Fig. 53.5) [53.50]. The simplest OLED is an electroluminescent compound sandwiched between metals of high and low work function, as depicted in Fig. 53.8. The anode electrode is normally indium tin oxide (ITO) as this material is semitransparent, allowing the light out of the device. On application of a voltage, electrons are injected from the low work function electrode into the lowest unoccupied molecular orbital (LUMO) level (conduction or π^* band in the case of an organic compound possessing a delocalised electron system) of the organic compound and holes from the high-work-function electrode into the highest occupied molecular orbital (HOMO) level (valence or π band in the case of an organic compound possessing a delocalised electron system). The recombination of these oppositely charged carriers then results in the emission of light. Work is focused on the use of low-molecular-weight organic molecules and polymers and there is considerable industrial interest in the application of such materials to various display technologies [53.51–54]. It is estimated that the global market for OLED displays will

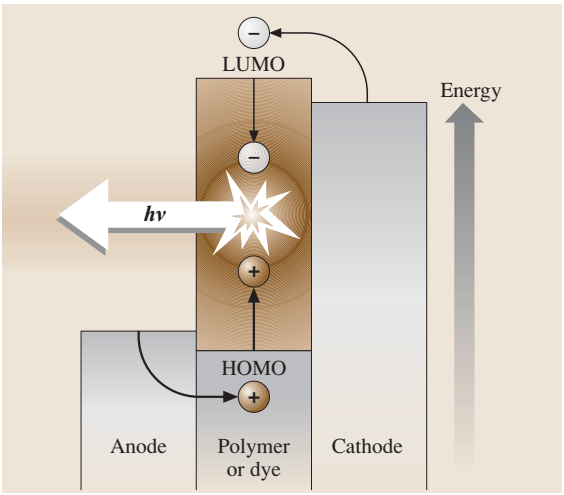

Fig. 53.8 Schematic energy band structure of an organic light-emitting device (OLED). The recombination of electrons and holes results in the emission of light of frequency ν and energy $h\nu$

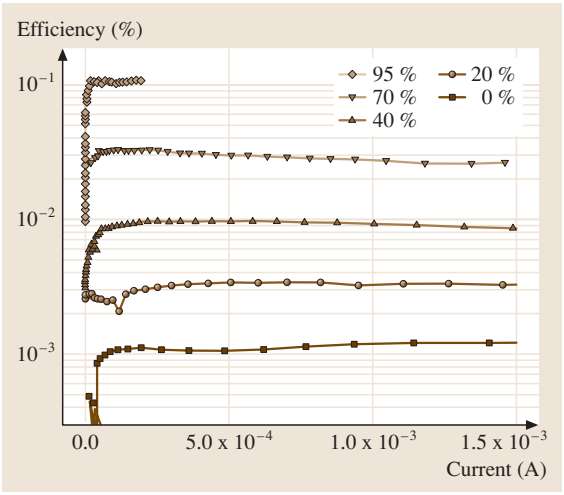

Fig. 53.9 External quantum efficiency versus current for OLEDs fabricated with MEH-PPV/DFD blended layers using blends with various concentrations (by weight) of DFD. (After *Ahn* et al. [53.56], with permission, © AIP)

increase from $112 million in 2003 to almost $2.3 billion by 2008 [53.55]. Organic light-emitting devices offer a number of advantages over liquid-crystal displays (LCDs) and the other technologies that currently dominate the flat-panel display market: OLEDs do not require backlighting and they can be made thinner and lighter. Furthermore, OLED displays provide higher contrast and truer colours, higher brightness, wider viewing angles, better temperature stability and faster response times than LCDs [53.54].

Many techniques have been used in attempts to optimise the performance of OLEDs. For example, a thin inorganic insulating layer such as LiF, or an organic monolayer may be inserted between the cathode and the emissive material [53.57, 58]. Electron- and hole-transporting layers can also be introduced between the cathode and the emitting layer and between the anode and the emitting layer, respectively, to improve and balance the injection of charge carriers [53.51]. As an alternative, OLEDs based on blended single layers of emissive and charge-transport materials may be fabricated [53.56, 59–61]. Such devices generally possess lower efficiencies than multilayer structures but they have the considerable advantage of ease of manufacture. Figure 53.9 shows how the external quantum efficiency of a blended layer OLED based on a polymer – poly[2,-(2-ethylhexyloxy)-5-methoxy-1,4-phenylenevinylene] (MEH-PPV) – and an electron-transport compound – 2,7-bis[2-(4-tert-butylphenyl)-1,3,5-oxadiazol-5-yl]-9,9-dihexylfluorene (DFD) – varies as the ratio MEH-PPV : DFD is changed in a spin-coated film [53.56]. The device efficiency increases with the amount of DFD so that the OLED fabricated with a 95% blend is about 100 times more efficient than that of pure MEH-PPV. For all the devices, the electroluminescence originates from the MEH-PPV material, indicating that the energy, or charge, transfer between the electron-transport compound and the polymer is very efficient.

Table 53.2 Performance of polymer-based organic light-emitting devices. (Data from Cambridge Display Technology [53.54])

Colour	Voltage (V)	Efficiency at 100 cd/m^2 (lm/W)	Measured lifetime at room temperature at fixed luminance (h) at (cd/m^2)
Red	3.6	1.5	1790 at 2000
Green	2.6	9.4	2867 at 2000
Blue	5.5	3.9	1426 at 720
Yellow	3.3	6.5	2420 at 4000

[a] All data taken using common cathode and may include an interlayer

When an electron and a hole recombine to form an excited molecular state in an organic material, the spins of the electrons in the excited and ground levels can either point in the same direction (triplet state) or in the opposite directions (singlet state). For quantum-mechanical reasons, 75% of recombination events are associated with triplet states which, in most cases, do not emit photons when they decay to the ground state. Hence, the production of emission from the triplet state of organic materials is a further means to improve the device efficiency [53.52, 62].

Table 53.2 shows some important parameters of polymer-based OLEDs with different colour outputs [53.54]. There is also a keen interest in developing white-light organic displays. For example, a large-area white-light-emitting OLED could provide a solid-state light source that might compete with conventional lighting technologies. Different methods of making an intrinsically white-emitting OLED by blending emissive species, either in single or multiple layers have been demonstrated [53.63–65]. Alternatively, a blue OLED can be used with one or more down-conversion layers [53.66].

53.3.3 Photovoltaic Devices

Concerns over global climate change, local air pollution and resource depletion are making photovoltaics (PVs) an increasingly attractive method of energy supply. The current technology is based on single-crystal silicon solar cells. These have developed since the 1940s and now possess conversion efficiencies of around 15% for commercial devices (although figures of around 25% are reported in the laboratory). However, the technology is more expensive than conventional power generation and there is much research on alternative materials. Photovoltaics using organic compounds, such as polymers or dyes, offer the possibility of large-scale manufacture at low temperature coupled with low cost. Until the end of the 20th century little progress had been made and energy conversion efficiencies of up to only about 1% were achieved. However, the availability of new conductive organic materials and different PV designs have significantly improved on this figure. To 2004, several laboratories have reported conversion efficiencies of 4–5%, with lifetimes of around 10^4 hours [53.67].

An organic solar cell device is very similar in structure to the OLED described in the previous section. If the incoming photons have energy greater than the band gap of the polymer (or greater than the HOMO–LUMO separation in the case of organic molecular materials) then the light will be absorbed, creating electrons and holes. In an inorganic photovoltaic cell, these electrons and holes would be generated within, or close to, a depletion region in the semiconductor and they would be free to migrate to opposite electrodes, where they can do useful work in an external electrical load. However, in the organic material the electrons and holes are bound together in excitons. An immediate problem in organic PV cells is to split these excitons. This can be conveniently done at an interface, the simplest being the junction between the electrodes and the organic material. Under open-circuit conditions, holes are collected at the high-work-function electrode (e.g. ITO) and electrons at the low-work-function electrode (e.g. Al). The open-circuit output voltage of the PV device depends on the work-function difference between the electrodes. Improvements in the efficiency of the exciton-splitting process can be achieved using organic compounds incorporating electron-donating and electron-accepting species. By creating interfaces of differing electron affinities, it is possible to enhance the probability of electron transfer between the molecules.

An alternative approach to organic PVs exploits a dye-sensitised solar cell, or Grätzel cell [53.68]. Here, the incoming photons are absorbed by molecules of a dye on a semiconductor surface with subsequent energy and electron transfer to the semiconductor. An electron is returned to the oxidised dye via an electrolyte. The efficiency of such devices can approach 10% [53.69].

53.3.4 Chemical Sensors

The development of effective devices for the identification and quantification of chemical and biochemical substances for process control and environmental monitoring is a growing need [53.70–72]. Many sensors do not possess the specifications to conform to existing or forthcoming legislation; some systems are too bulky/expensive for use in the field. Inorganic materials such as the oxides of tin and zinc have traditionally been favoured as the sensing element [53.73]. However, one disadvantage of sensors based on metallic oxides is that they usually have to be operated at elevated temperatures, limiting some applications. As an alternative, there has been considerable interest in trying to exploit the properties of organic materials. Many such substances, in particular phthalocyanine derivatives, are known to exhibit a high sensitivity to gases [53.74]. Lessons can also be taken from the biological world; one household carbon-monoxide detector is designed to simulate the reaction between CO and haemoglobin. A significant advantage of organic compounds is that their sensitivity and selectivity can be tailored to a particular application by modifications to their chemical structure. Moreover, thin-film technologies, such as self-assembly or layer-by-layer electrostatic deposition, enable ultrathin layers of organic materials to be engineered at the molecular level [53.75].

There are many physical principles upon which sensing systems might be based; changes in electrical resistance (chemiresistors), refractive index (fibre-optic sensors) and mass (quartz microbalance) have all been exploited in chemical sensing. The main challenges in the development of new sensors are in the production of cheap, reproducible and reliable devices with adequate sensitivities and selectivities.

A simple chemiresistor sensor exploits the resistance change of a thin layer of a gas-sensitive material. For example, the conductivity of phthalocyanine thin films can be changed in the presence of oxidising or reducing gases [53.76]. This effect is analogous to the doping of an inorganic semiconductor, such as silicon, with acceptor or donor impurities (Sect. 53.1.3). A problem associated with these chemiresistor devices is that the current outputs are low (typically picoamperes) requiring elaborate

detection electronics and careful shielding and guarding of components. This difficulty may be overcome by incorporating the organic sensing layer into a silicon field-effect transistor. A schematic diagram of such a structure is shown in Fig. 53.10 [53.77, 78]. Changes in the sheet resistance of the sensing layer are reflected in the variation in both the amplitude and phase of the transfer function of the device. These devices have been shown to respond well to low (vapour parts per million) concentrations of NO_2 [53.79]. It is also possible to use a chemically sensitive organic film as the semiconductive layer in a diode or a transistor. In these cases the device must be fabricated so that the gas can interact readily with the organic material.

While many sensing devices show adequate sensitivities, the selectivity can be poor. For example, a semiconductive polymer may show a similar change in electrical resistance to a range of oxidising (reducing) gases. To get around this difficulty, one approach that is being embraced enthusiastically by researchers is to use an array of sensing elements, rather than a single device. This is the method favoured by nature. The human olfactory system has many receptors cells (sensors), which are individually nonspecific; signals from these are fed to the brain via a network of primary and secondary neurons for processing. It is generally believed that the selectivity of the olfactory system is a result of a high degree of parallel processing in the neural architecture. Artificial neural networks can emulate the connectivity of the olfactory neurons. The electronic nose is an attempt to mimic the human olfactory system and there are now several companies marketing such equipment [53.80]. Individual sensors can be based on polymer films. Each element is treated in a slightly different way during deposition so that it responds uniquely on exposure to a particular gas or vapour. The pattern of resistance changes in the sensor array can then be used to fingerprint the vapour.

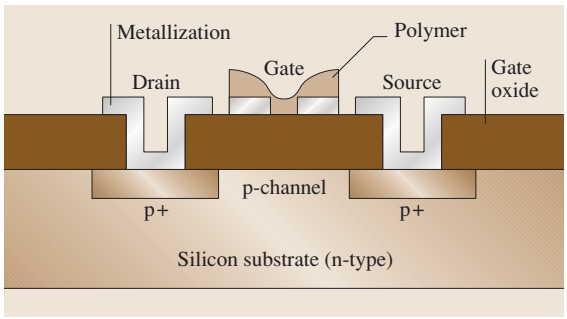

Fig. 53.10 Structure of hybrid silicon/organic field-effect transistor for chemical sensing. (After *Barker* et al. [53.78])

53.4 Molecular-Scale Electronics

53.4.1 Moore's Laws

The second strand to molecular electronics (molecular-scale electronics) recognises the spectacular size reduction in the individual processing elements in integrated circuits over recent years. The first microprocessor chip manufactured in 1972 by Intel (8008) had a clock speed of 200 kHz and contained 3500 transistors. There are 55 million transistors on the Pentium® 4 chip (November, 2002), fabricated using 0.13-μm process technology, and operating at a clock speed of 3 GHz.

Moore's law (or Moore's first law) states that the functions per chip double every 1.5 years. This will probably describe developments over at least the next decade. The semiconductor industries have produced an international technology roadmap for the future of complementary metal oxide semiconductor (CMOS) technology [53.81]. Figure 53.11 shows the anticipated growth in the density of the transistors in both the microprocessor unit (MPU) and the dynamic random-access memory (DRAM) of a CMOS chip over the next decade.

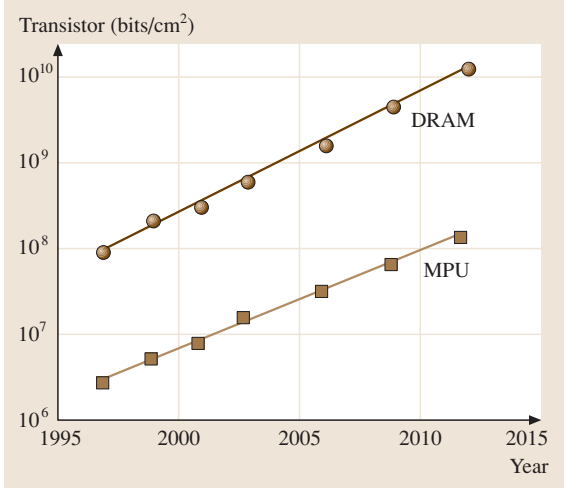

Fig. 53.11 Predicted feature size in CMOS devices. (After [53.81])

Table 53.3 Information content for various *applications*. (After *Tour* [53.3])

Application	Typical information content (bytes)
Color photograph	10^5
Average book	10^6
Desktop computer	10^8
Genetic code	10^{10}
Human brain	10^{13}
Library of congress	10^{15}

The prediction is for a 30-nm minimum feature size (gate length) for the MPU and 10^{10} transistors per cm^2 in the case of the memory by the year 2012. These figures are regularly updated. This device density is remarkable and provides the means to store significant amounts of data, Table 53.3 [53.3]. However, molecular-scale electronics has the potential for further increases in device density. For example, using ~1–3 nm organic molecules as the processing elements, 10^{13}–10^{14} 'devices' could be fitted into 1 cm^2 [53.3].

There are, however, a number of technological problems issues that will need to be overcome for the predictions for the CMOS-based roadmap to be realised [53.82]. Not least, are the materials limitations of the silicon/silicon dioxide system. For example, charge leakage becomes a problem when the insulating silicon dioxide layers are thinned to a few nm. Heat dissipation is another key factor. A Pentium® 4 chip, with 10^7–10^8 transistors operating at the current nanosecond rate can emit 50–60 W of heat. Financial issues are also problematic as ever more complex integrated circuits are produced. Intel's Fab 22, a chip-fabrication facility (FAB) which opened in Chandler, Arizona in October 2001, cost $2 billion to construct and equip. The cost of building a fab is projected to rise to $15–30 billion by 2010 and could be as much as $200 billion by 2015 [53.83]. This significant increase in cost (Moore's second law) is due to the extremely sophisticated tools that will be needed to form the increasingly small features of the devices. Molecular-scale technology will, of course, also need to address such problems – plus many more.

53.4.2 Nanoscale Organic Films

Before organic molecules can be exploited in device architectures (i. e. those familiar from Si-based microelectronics) ways must be found to deposit them onto surfaces. Well-established methods of organic film deposition include electrodeposition, thermal evaporation and spinning [53.84]. The Langmuir–Blodgett (LB) technique, self-assembly and layer-by-layer electrostatic deposition are further means for producing layers of organic materials. These allow ultrathin-film assemblies of organic molecules to be engineered at the molecular level and are of particular relevance to molecular-scale electronics [53.85, 86].

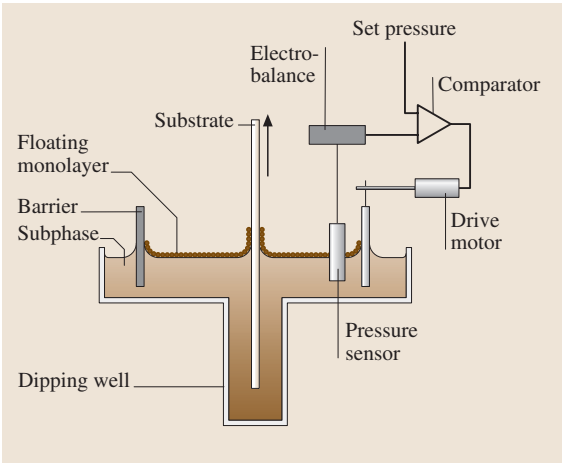

Fig. 53.12 System for the deposition of Langmuir–Blodgett films

Langmuir–Blodgett films are prepared by first depositing a small quantity of an amphiphilic compound (i. e. one containing both polar and nonpolar groups) dissolved in a volatile solvent onto the surface of purified water [53.86, 87]. The classical materials are long-chain fatty acids, such as *n*-octadecanoic acid (stearic acid). When the solvent has evaporated, the organic molecules may be organised into a floating two-dimensional *crystal* by compression on the water surface. As the area available to the organic molecules is reduced, the floating film will undergo several phase transformations. These are, to a first approximation, analogous to three-dimensional gas, liquid and solid phases. The phase changes may readily be identified by monitoring the surface pressure as a function of the area occupied by the molecules in the film. This is the two-dimensional equivalent to the pressure-versus-volume isotherm for a gas. In the *gaseous* state the molecules are far enough apart on the water surface that they exert little force on one another. As the surface area of the monolayer is reduced, the hydrocarbon chains will begin to interact. The *liquid* state that is formed is generally called the expanded monolayer phase. The hydrocarbon chains of the molecules in such a film are in a random, rather than regular orienta-

tion, with their polar groups in contact with the subphase. As the molecular area is progressively reduced, condensed phases may appear. There may be more than one of these and the emergence of each condensed phase can be accompanied by constant-pressure regions of the isotherm, as observed in the cases of a gas condensing to a liquid and a liquid solidifying. In the condensed monolayer states, the molecules are closely packed and are oriented with their hydrocarbon chain pointing away from the water surface. The area per molecule in such a state will be similar to the cross-sectional area of the hydrocarbon chain, i. e. $\approx 0.19\,\mathrm{nm}^2$/molecule.

If the surface pressure is held constant in one of the condensed phases, then the film may be transferred from the water surface onto a suitable solid substrate simply by raising and lowering the latter through the monolayer–air interface. Figure 53.12 shows a schematic diagram of the equipment required for LB film deposition. In this technique, introduced by Langmuir and Blodgett [53.86] the floating condensed monolayer is transferred, like a carpet, as the substrate is raised and/or lowered through the air/monolayer interface. A number of different LB deposition *modes* are possible. The most commonly encountered situation is Y-type deposition, which refers to monolayer transfer on both the upward and downward movements of the substrate. Instances in which the floating monolayer is only transferred to the substrate as it is being inserted into the subphase, or only as it is being removed, are also observed. These deposition modes are called X-type and Z-type deposition, respectively.

Self-assembly is a much simpler process than that of LB deposition. Monomolecular layers are formed by the immersion of an appropriate substrate into a solution of the organic material [53.85]. The best known examples of self-assembled systems are organosilicon on hydroxylated surfaces (SiO_2, Al_2O_3, glass etc.) and alkanethiols on gold, silver and copper. However, other combinations include: dialkyl sulphides on gold; dialkyl disulphides on gold; alcohols and amines on platinum; and carboxylic acids on aluminium oxide and silver. The self-assembly process is driven by the interactions between the head group of the self-assembling molecule and the substrate, resulting in a strong chemical bond between the head group and a specific surface site, e.g. a covalent Si−O bond for alkyltrichlorosilanes on hydroxylated surfaces.

The combination of the self-assembly process with molecular recognition offers a powerful route to the development of nanoscale systems that may have technological applications as chemical sensing or switching devices. For instance, the complexation of a neutral or ionic guest at one site in a molecule may induce a change in the optical or redox properties of the system. Monolayers containing both an electroactive TTF unit and a metal-binding macrocycle assembled onto platinum have been shown to exhibit electrochemical recognition to Ag^+ ions [53.88].

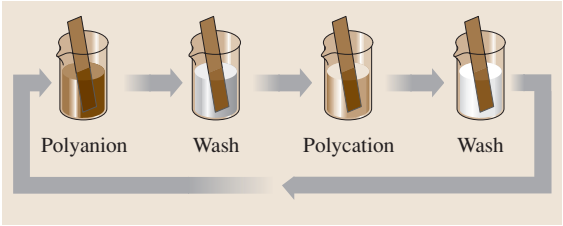

Fig. 53.13 Deposition of layer-by-layer polyelectrolyte films by the sequential immersion of a solid substrate in solutions of the polyanions and polycations

The self-assembly process, as described above, is usually restricted to the deposition of a single molecular layer on a solid substrate. However, chemical means can be exploited to build up multilayer organic films. A method pioneered by Sagiv is based on the successive absorption and reaction of appropriate molecules [53.89, 90]. The head groups react with the substrate to give a permanent chemical attachment and each subsequent layer is chemically attached to the one before in a very similar way to that used in systems for supported synthesis of proteins.

Another technique for building up thin films of organic molecules is driven by the ionic attraction between opposite charges in two different polyelectrolytes, the so-called *layer-by-layer* assembly technique [53.91–93]. A solid substrate with a positively charged planar surface is immersed in a solution containing an anionic polyelectrolyte and a monolayer of polyanion is adsorbed, Fig. 53.13. Since the adsorption is carried out at relatively high concentrations of the polyelectrolyte, most of the ionic groups remain exposed to the interface with the solution and thus the surface charge is reversed. After rinsing in pure water, the substrate is immersed in a solution containing the cationic polyelectrolyte. Again, a monolayer is adsorbed but now the original surface charge is restored, resulting in the formation of a multilayer assembly of both polymers. It is possible to use a sensitive optical technique, such as surface plasmon resonance to monitor, in situ, the growth of such electrostatically assembled films [53.94]. The layer-by-layer method has been used to build up layers of conductive poly-

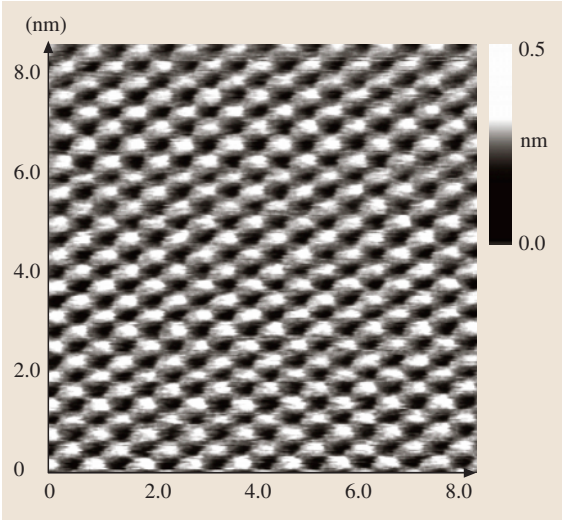

Fig. 53.14 Atomic force micrograph of a 12-layer, *n*-eicosanoic-acid Langmuir–Blodgett film deposited onto silicon. (After, in part, with permission from *Evanson* et al. [53.98]. © (1996) ACS)

mers, e.g. partially doped polyaniline and a polystyrene polyanion [53.95]. Biocompatible surfaces consisting of alternate layers of charged polysaccharides and oppositely charged synthetic polymers can also be deposited in this way [53.96]. A related, but alternative, approach uses layer-by-layer adsorption driven by hydrogen-bonding interactions [53.97].

The organisation of the organic molecules in multilayer assemblies may be investigated by a number of analytical techniques including X-ray and neutron reflection, electron diffraction and infrared spectroscopy [53.86]. Figure 53.14 shows an example of an atomic force micrograph of a 12-layer *n*-eicosanoic acid LB film deposited onto single-crystal silicon [53.98]. Lines of individual molecules are evident at the magnification shown. Figure 53.15 contrasts the molecular organisation expected in an LB multilayer with that in electrostatically deposited layer-by-layer films. For the latter case, the polyelectrolyte chains within each layer will become entangled, and may even penetrate into the layers above and below, leading to a less-ordered film than that produced by LB deposition.

53.4.3 Patterning Technologies

The problem of connecting together the individual processing elements in any future molecular computer is challenging. Each one of the 55 million transistors in the

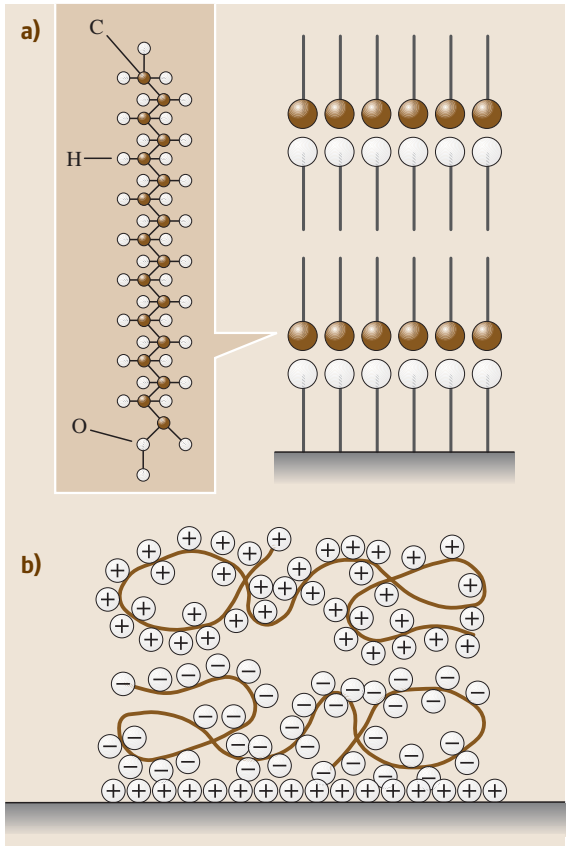

Fig. 53.15a,b Molecular organisation in **(a)** a Langmuir–Blodgett multilayer assembly and **(b)** a polyelectrolyte multilayer deposited by the electrostatic method

Pentium® 4 chip is addressable and connected to a power supply. Organic molecules can be difficult to arrange on a surface or in a three-dimensional array such that each molecule is addressable. Planar inorganic materials are normally patterned using photolithography. Here, a surface is first covered with a light-sensitive photoresist, which is exposed to ultraviolet light through a contact mask. Either the exposed photoresist (positive resist) or the unexposed regions (negative resist) can then be developed to leave a positive or negative image of the mask on the surface. This approach is routinely used in the fabrication of devices based on inorganic semiconductors. However, difficulties can be encountered when used with organic films, as the photoresists themselves are based on organic compounds.

Brittain et al. [53.99] describe a series of *soft* lithographic methods that may be better suited to the patterning of organic layers. Pouring a liquid polymer,

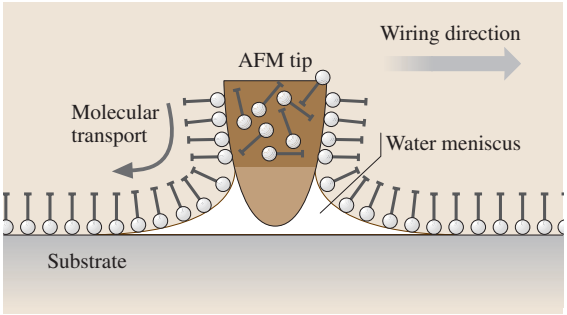

Fig. 53.16 Dip-pen patterning showing the transfer of an *ink* onto *paper* using the tip of an atomic force microscope. (After *Piner* et al. [53.100])

such as polydimethylsiloxane (PDMS) onto a *master* made from silicon forms a pattern-transfer element. The polymer is allowed to cure to form an elastomer, which can then be removed from the master. This replica can subsequently be used as a stamp to transfer chemical ink, such as a solution of an alkanethiol, to a surface.

Scanning microscopy methods offer a powerful means of manipulating molecules. Careful control of an atomic force microscope (AFM) tip can allow patterns to be drawn in an organic film [53.101, 102]. Such techniques can also be used to reposition molecules, such as the fullerene C_{60}, on surfaces and to break up an individual molecule [53.103]. A further approach that has recently been developed is called dip-pen nanolithography (DPN) [53.100], Fig. 53.16. This is able to deliver organic molecules in a positive printing mode. An AFM tip is used to *write* alkanethiols on a gold thin film in a manner analogous to that of a fountain pen. Molecules flow from the AFM tip to a solid substrate (*paper*) via capillary transport, making DPN a potentially useful tool for assembling nanoscale devices. Recent developments of DPN have included an overwriting capability that allows one nanostructure to be generated and the areas surrounding that nanostructure to be filled with a second type of ink [53.104]. Perhaps the greatest limitation in using scanning probe methodologies for ultrahigh-resolution nanolithography over large areas derives from the serial nature of most techniques. However, an eight-pen nanoplotter capable of doing parallel lithography has been reported [53.105]. The DPN method has also been used to deposit magnetic nanostructures [53.106] and arrays of protein molecules [53.107].

The need to combine large-area coatings with device patterning has resulted in the development of direct-write fabrication methods, such as ink-jet printing [53.108–110]. Although ink-jet printhead droplet ejection can be achieved with thermal (bubble-jet) and piezoelectric modes of operation, the majority of published literature on ink-jet printing as a tool for manufacturing organic devices has been the result of using piezoelectric-actuated printers. Piezoelectric printhead technology is favoured primarily because it applies no thermal load to the organic *inks* and is compatible with the printing of digital images. The combination of solution-processable emissive polymers with ink-jet printing offers some promise in the development of low-cost high-resolution displays [53.111]. The technique has also been applied to the manufacture of all-polymer transistor circuits [53.112, 113].

53.4.4 Molecular Device Architectures

The *bottom-up* approach to molecular electronics offers many intriguing prospects for manipulating materials on the nanometre scale, thereby providing opportunities to build up novel architectures with predetermined and unique physical and/or chemical properties. Two relatively simple examples of organic superlattice structures are the incorporation of an electric polarisation into a multilayer array to form thin films exhibiting pyroelectric behaviour [53.114] and the use of non-centrosymmetric layers for second-order nonlinear optical response, e.g. second-harmonic generation [53.115]. In both instances, the multilayer thin films can be built up using the LB approach.

To realise functional nanoelectronic circuits, a number of workers have investigated the electrical characteristics of structures in which organic molecules are sandwiched between two metallic electrodes. Of particular interest is the possibility of observing molecular rectification using monolayer or multilayer films. This follows the prediction [53.116] that an asymmetric organic molecule containing a donor and an acceptor group separated by a short σ-bonded bridge, allowing quantum-mechanical tunnelling, should exhibit diode characteristics. There have been many attempts to demonstrate this effect in the laboratory, particularly in organic thin films [53.117–119]. Asymmetric current-versus-voltage behaviour has certainly been recorded for many metal/insulator/metal structures, although these results are often open to several interpretations as a result of the asymmetry of the electrode configuration.

In other cases *switching* behaviour has been reported [53.3–8, 12, 13, 119]. As with the work on molecular rectification, the origin of the switching is not always clear. For example, is this a property of the organic molecules, the metallic electrode or of the

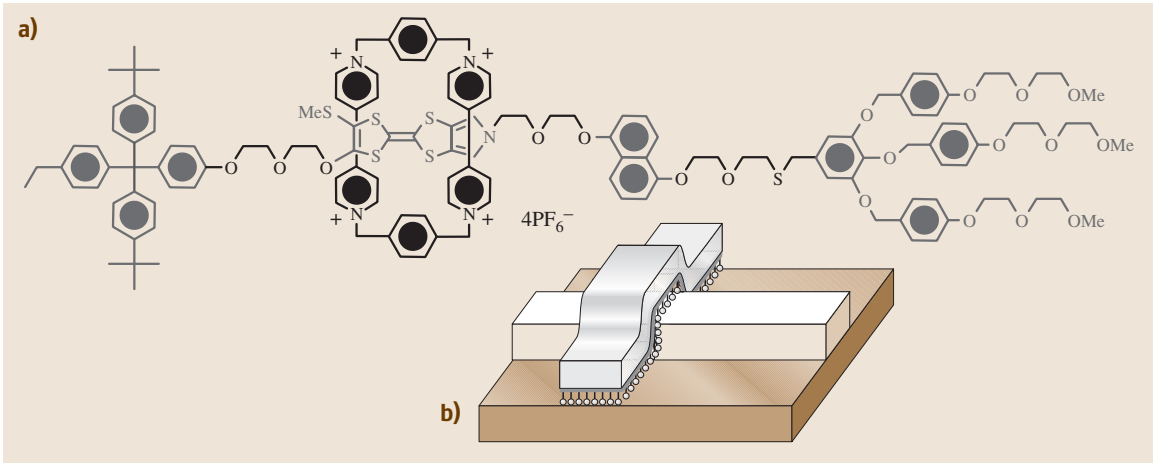

Fig. 53.17 (a) Bistable rotaxane. (b) Schematic diagram of cross-wire structure for switching studies. (After *Chen* et al. [53.5])

presence of any interfacial (e.g. oxide) layer (or a combination of these)? Bistable rotaxane molecules have been used as the basis of some of these studies, an example is shown in Fig. 53.17a. This molecule is amphiphilic and the ring component can move between the polar and nonpolar regions of the main part of the molecule. The molecules can be assembled on an electrode using the LB approach and a top electrode then deposited to form the crossbar structure shown in Fig. 53.17b [53.5–7]. Alternatively, the molecules can be solution-cast between Pt source and drain electrodes (with gaps of 1–2 nm) in transistor structures [53.9]. In some of the experiments, the absence of switching using *control* compounds suggests that the rotaxane molecule itself is responsible for the bistability [53.7]. Such results augur well for the development of molecular-scale logic circuitry.

Nanoscale organic devices can also exploit charge storage on nanoparticles or at interfaces. One important metal oxide semiconductor (MOS) device is the flash memory [53.120]. This is similar in structure to a MOS field-effect transistor (MOSFET), except that it has two gate electrodes, one on top of the other. The top electrode forms the control gate, below which a *floating gate* is capacitively coupled to the

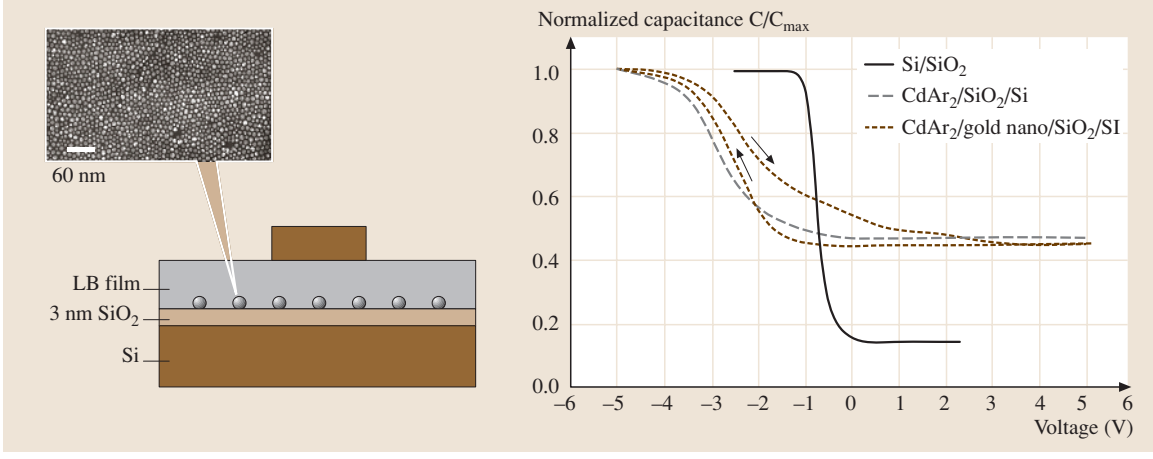

Fig. 53.18 *Left*: metal–insulator–semiconductor (MIS) structure incorporating gold nanoparticles; a transmission electron micrograph of the nanoparticles is shown. *Right*: normalised capacitance versus voltage characteristics for different MIS devices. (After *Paul* et al. [53.10], © (2003) ACS)

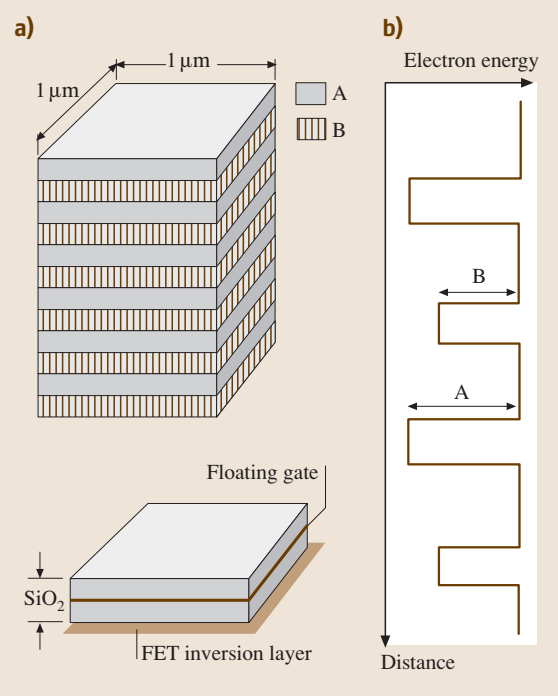

Fig. 53.19 **(a)** Molecular memory holding N bits (*top*) compared to a conventional silicon memory holding 1 bit (*bottom*). **(b)** Electron energy versus perpendicular distance for molecular memory with no applied electric field. (After *Burrows* et al. [53.123], with permission, © Elsevier [123])

control gate and the underlying silicon. The memory cell operation involves putting charge on the floating gate or removing it, corresponding to two logic levels. Nanoflash devices utilise single or multiple nanoparticles as the charge-storage elements. These are usually embedded in the gate oxide of a field-effect transistor and located in close proximity (2–3 nm) to the transistor channel [53.121]. Figure 53.18 shows the characteristics of a memory device incorporating metallic nanoparticles deposited by the LB technique [53.10]. The device structure is shown schematically in the figure. The gold nanoparticles (Q-Au) were of nominal diameter 10 nm and passivated with an organic capping layer. Cadmium arachidate ($CdAr_2$) LB layers were used to provide an insulating gate layer. Figure 53.18 also shows the normalised capacitance versus voltage ($C-V$) data, measured at 1 MHz and at a voltage scan rate of 40 mV/s for three different device structures: Al/SiO_2/p-Si; Al/20 LB layers $CdAr_2$/SiO_2/p-Si; and Al/20 LB layers $CdAr_2$/one LB layer Q-Au/p-Si. The C–V curve for the reference Al/SiO_2/Si sample reveals the usual accumulation/depletion/inversion characteristics associated with metal–insulator–semiconductor (MIS) structures, with a flat-band voltage of approximately −1 V. Negligible hysteresis was evident on reversing the voltage scan. The data for the Si/SiO_2/$CdAr_2$ structure also show clear accumulation, depletion and inversion regions, again with no hysteresis on reversing the direction of the voltage scan. The most significant difference in the structures with and without the Q-Au nanoparticles is the relatively large hysteresis in the MIS structure containing the Q-Au layer. This was thought to be indicative of charge storage in the gold nanoparticles [53.10]. In a somewhat different approach, the same group has used a self-assembly technique to chemically attach gold nanoparticles to a SiO_2 surface [53.122]. When incorporated into a transistor structure, the resulting device was shown to behave as a nonvolatile electrically erasable programmable read-only memory.

Molecular-scale electronics may also offer increased device densities by fabricating three-dimensional architectures. In 1989, the principle of a three-dimensional memory based on LB films was described [53.123]. The device requires a molecule with a central conjugated region of high electron affinity (for an n-type material, the electron affinity is the energy difference between the bottom of the conduction band and the vacuum level) surrounded by aliphatic substituents of low electron affinity, A multilayer structure, as shown in Fig. 53.19, could be used to store one N-bit word, the presence or absence of charge on the n-th layer representing a 0 or 1 of the n-th bit. The LB film could be assembled on the gate of an FET and, on application of an electric field, transport of bits across the layers may be detected as induced charge on the gate.

53.5 DNA Electronics

The study of the electronic behaviour of organic compounds has led some scientists to work on the electrical properties of biological materials. Deoxyribonucleic acid (DNA) is arguably the most significant molecule in nature. It may also be an important material for molecular electronics applications. Reports into the

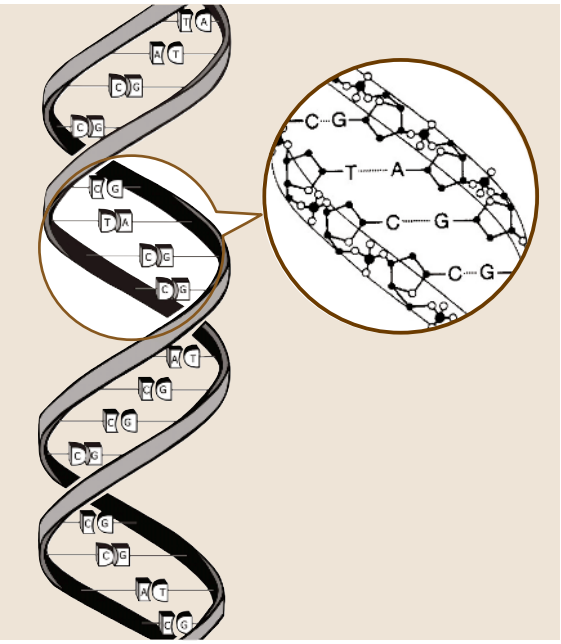

Fig. 53.20 DNA double helix showing the position of the four bases: guanine (G), cytosine (C), adenine (A) and thymine (T)

electronic properties of DNA have already generated controversy in the literature [53.16, 124–128]. According to some, DNA is a molecular wire of very small resistance. Others, however, find that DNA behaves as an insulator. These seemingly contradictory findings can probably be explained by the different DNA sequences and experimental conditions used to monitor the conductivity [53.16].

The DNA strand in the double-helix arrangement consists of a long polymer backbone consisting of repeating sugar molecules and phosphate groups, Fig. 53.20. Each sugar group is attached to one of four bases, guanine (G), cytosine (C), adenine (A) and thymine (T). The chemical bonding is such that an A base only ever pairs with a T base, while a G always pairs with a C. Some of the electron orbitals belonging to the bases overlap quite well with each other along the long axis of the DNA. This provides a path for electron transfer along the molecule, in a similar fashion to the one-dimensional conduction seen in conjugated polymers, Sect. 53.1.2.

Theoretical and experimental work now suggests that a hole (i. e. a positive charge) is more stable on a G–C base pair than on an A–T base pair [53.16]. The energy difference between these two pairs is substantially larger than the thermal energy of the charge carrier. Under these conditions, a hole will localise on a particular G–C base pair. Because the A–T base pairs have a higher energy, they act as a barrier to hole transfer. However, if the distance between two G–C base pairs is small enough, the hole can tunnel quantum-mechanically from one pair to the next. In this way, charge carriers are able to shuttle along a single DNA molecule over a distance of a few nanometres.

DNA chips exploit the fact that short strands of DNA will bind to other segments of DNA that have complementary sequences, and can therefore be used to probe whether certain genetic codes are present in a given specimen of DNA. Microfabricated chips with many parallel DNA probes are becoming widespread in analytical and medical applications. Currently, the chips are read out optically, but further miniaturisation might require new read-out schemes, possibly involving the electron-transfer properties of DNA.

Computations by chemical or biological reactions overcome the problem of parallelism and interconnections in a classical system. If a string of DNA can be put together in the right sequence, it can be used to solve combinational problems. The calculations are performed in test tubes filled with strands of DNA. Gene sequencing is used to obtain the result. For example, *Adleman* [53.129] calculated the *travelling-salesman problem* to demonstrate the capabilities of DNA computing. DNA computing on parallel problems potentially provides 10^{14} millions of instructions per second (MIPS) and uses less energy and space than conventional supercomputers. While CMOS supercomputers operate 10^9 operations per Joule, a DNA computer could perform about 10^{19} operations per Joule. Data could potentially be stored on DNA in a density of approximately 1 bit per nm^3 while existing storage media such as DRAMs require 10^{12} nm^3 to store 1 bit.

53.6 Conclusions

Organic compounds possess a wide range of fascinating physical and chemical properties that make them attractive candidates for exploitation in electronic and optoelectronic devices. It is not, however, anticipated that these materials will displace silicon in the foreseeable future as the dominant material for fast signal

processing. It is much more likely that organic materials will find use in other niche areas of electronics, where silicon and other inorganic semiconductors cannot compete. Examples already exist, such as liquid-crystal displays and certain chemical sensors. Organic light-emitting structures are likely to make a major impact in the marketplace over the next ten years.

Over the first decades of the 21st century, classical CMOS technology will come up against a number of technological barriers. The bottom-up approach to molecular electronics provides an alternative and attractive way forward and, as such, it is currently an area of exciting interdisciplinary activity. However, the challenges in fabricating molecular switches and connecting them together are formidable. Living systems use a different approach; these assemble themselves naturally from molecules and are extremely energetically efficient when compared with man-made computational devices. More radical approaches to materials fabrication and device design, exploiting self-organisation, may be needed to realise fully the potential offered by molecular-scale electronics.

References

53.1 M. C. Petty, M. R. Bryce, D. Bloor (eds): *An Introduction to Molecular Electronics* (Edward Arnold, London 1995)
53.2 T. H. Richardson (ed): *Functional Organic and Polymeric Materials* (Wiley, Chichester 2000)
53.3 J. M. Tour: *Molecular Electronics* (World Scientific, New Jersey 2003) Chap. 2
53.4 P. E. Kornilovitch, A. M. Bratkovsky, R. S. Williams: Phys. Rev. B **66**, 245413 (2002)
53.5 Y. Chen, G.-Y. Jung, D. A. A. Ohlberg, X. Li, D. R. Stewart, J. O. Jeppesen, K. A. Nielsen, J. F. Stoddart, R. S. Williams: Nanotechnology **14**, 462 (2003)
53.6 Y. Chen, D. A. A. Ohlberg, X. Li, D. R. Stewart, R. S. Williams, J. O. Jeppesen, K. A. Nielsen, J. F. Stoddart, D. L. Olynick, E. Anderson: Appl. Phys. Lett. **82**, 1610 (2003)
53.7 M. R. Diehl, D. W. Steuerman, H.-R. Tseng, S. A. Vignon, A. Star, P. C. Celestre, J. F. Stoddart, J. R. Heath: ChemPhysChem **4**, 1335 (2003)
53.8 L. Ma, S. Pyo, J. Ouyang, Q. Xu, Y. Yang: Appl. Phys. Lett. **82**, 1419 (2003)
53.9 H. Yu, Y. Luo, K. Beverly, J. F. Stoddart, H.-R. Tseng, J. R. Heath: Angew. Chem. **42**, 5706 (2003)
53.10 S. Paul, C. Pearson, A. Molloy, M. A. Cousins, M. Green, S. Kolliopoulou, P. Dimitrakis, P. Normand, D. Tsoukalas, M. C. Petty: Nano. Lett. **3**, 533 (2003)
53.11 J. M. Tour, L. Cheng, D. P. Nackashi, Y. Yao, A. K. Flatt, S. K. St. Angelo, T. E. Mallouk, P. D. Franzen: J. Am. Chem. Soc. **125**, 13279 (2003)
53.12 L. D. Bozano, B. W. Kean, V. R. Deline, J. R. Salem, J. C. Scott: Appl. Phys. Lett. **84**, 607 (2004)
53.13 J. Ouyang, C.-W. Chu, C. R. Szmanda, L. Ma, Y. Yang: Nature Mater. **3**, 918 (2004)
53.14 R. M. Metzger: J. Solid State Chem. **168**, 696 (2002)
53.15 J. Chen, W. Wang, M. A. Reed, A. M. Rawlett, D. W. Price, J. M. Tour: Appl. Phys. Lett. **77**, 1224 (2000)
53.16 C. Dekker, M. A. Ratner: Phys. World **14**, 29 (2001)
53.17 K. E. Drexler: *Nanosystems: Molecular Machinery, Manufacturing and Computation* (Wiley, New York 1992)
53.18 C. Nicolini (ed.): *Molecular Manufacturing* (Plenum, New York 1996)
53.19 S. Roth: *One-Dimensional Metals* (VCH, Weinheim 1995)
53.20 C. D. Dimitrakopoulos, D. J. Mascaro: IBM J. Res. Devel. **45**, 11 (2001)
53.21 M. R. Bryce, M. C. Petty: Nature **374**, 771 (1995)
53.22 W. J. Feast, J. Tsibouklis, K. L. Pouwer, L. Groenendaal, E. W. Meijer: Polymer **37**, 5017 (1996)
53.23 J. R. Ferraro, J. M. Williams: *Introduction to Synthetic Electrical Conductors* (Academic, Orlando 1987)
53.24 J. D. Wright: *Molecular Crystals* (Cambridge Univ. Press, Cambridge 1995)
53.25 H. W. Kroto, D. R. M. Walton (eds): *The Fullerenes* (Cambridge Univ. Press, Cambridge 1993)
53.26 G. Timp (ed.): *Nanotechnology* (Springer, Berlin Heidelberg New York 1998)
53.27 R. Saito, G. Dresselhaus, M. S. Dresselhaus: *Physical Properties of Carbon Nanotubes* (Imperial College Press, London 1998)
53.28 L. Duclaux: Carbon **40**, 1751 (2002)
53.29 P. May: Phys. World **8**, 52 (1995)
53.30 Plastic Logic, Cambridge, UK (2005): http://www.plasticlogic.com/
53.31 S. R. Forrest: Nature **428**, 911 (2004)
53.32 E. H. Rhoderick: *Metal–Semiconductor Contacts* (Clarendon, Oxford 1978)
53.33 Y. L. Hua, M. C. Petty, G. G. Roberts, M. M. Ahmad, M. Hanack, M. Rein: Thin Solid Films **149**, 161 (1987)
53.34 G. Horowitz: Adv. Mater. **2**, 286 (1990)
53.35 H. E. Katz: J. Mater. Chem. **7**, 369 (1997)
53.36 S. Scheinert, G. Paasch: Phys. Status Solidi (a) **201**, 1263–1301 (2004)
53.37 A. R. Brown, A. Pomp, C. M. Hart, D. M. de Leeuw: Science **270**, 972 (1995)

53.38 J. G. Laquindanum, H. E. Katz, A. J. Lovinger, A. Dodabalapur: Chem. Mater. **8**, 2542 (1996)
53.39 Z. Bao, A. J. Lovinger, A. Dodabalapur: Adv. Mater. **9**, 42 (1997)
53.40 C. D. Dimitrakopoulos, B. K. Furman, T. Graham, S. Hegde, S. Purushothaman: Synth. Met. **92**, 47 (1998)
53.41 C. D. Dimitrakopoulos, S. Purushothaman, J. Kymissis, A. Callegari, J. M. Shaw: Science **283**, 822 (1999)
53.42 H. Sirringhaus, T. Kawase, R. H. Friend, T. Shimoda, M. Inbasekaran, W. Wu, E. P. Woo: Science **290**, 2123 (2000)
53.43 H. Klauk, M. Halik, U. Zschieschang, F. Eder, G. Schmid, C. Dehm: Appl. Phys. Lett. **82**, 4175 (2003)
53.44 J. Lee, K. Kim, J. H. Kim, S. Im, D.-Y. Jung: Appl. Phys. Lett. **82**, 4169 (2003)
53.45 P. F. Baude, D. A. Ender, M. A. Haase, T. W. Kelley, D. V. Muyres, S. D. Theiss: Appl. Phys. Lett. **82**, 3964 (2003)
53.46 M. S. Fuhrer, B. M. Kim, T. Durkop, T. Brintlinger: Nano. Lett. **2**, 755 (2002)
53.47 A. Javey, Q. Wang, A. Ural, Y. M. Li, H. J. Dai: Nano. Lett. **2**, 929 (2002)
53.48 F. Léonard, J. Tersoff: Phys. Rev. Lett. **88**, 258302–1 (2002)
53.49 K. Tsukagoshi, N. Yoneya, S. Uryu, Y. Aoyagi, A. Kanda, Y. Ootuka, B. W. Alphenaar: Physica B **323**, 107 (2002)
53.50 J. H. Burroughes, D. D. C. Bradley, A. R. Brown, R. N. Marks, K. Mackay, R. H. Friend, P. L. Burns, A. B. Holmes: Nature **347**, 359 (1990)
53.51 S. Miyata, H. S. Nalwa (eds): *Organic Electroluminescent Materials and Devices* (Gordon Breach, Amsterdam 1997)
53.52 A. J. Hudson, M. S. Weaver: Organic electroluminescence. In: *Functional Organic and Polymeric Materials*, ed. by T. H. Richardson (Wiley, Chichester 2000) p. 365
53.53 R. Farchioni, G. Grosso (eds): *Organic Electronic Materials* (Springer, Berlin, Heidelberg 2001)
53.54 Cambridge Display Technology (data provided February 2005): http://www.cdtltd.co.uk/
53.55 J. K. Borchardt: Mater. Today **7**, 42 (Sept. 2004)
53.56 J. H. Ahn, C. Wang, C. Pearson, M. R. Bryce, M. C. Petty: Appl. Phys. Lett. **85**, 1283 (2004)
53.57 L. S. Hung, C. W. Tang, M. G. Mason: Appl. Phys. Lett. **70**, 152 (1997)
53.58 G.-Y. Jung, C. Pearson, L. E. Horsburgh, I. D. W. Samuel, A. P. Monkman, M. C. Petty: J. Phys. D: Appl. Phys. **33**, 1029 (2000)
53.59 Y. Cao, I. D. Parker, G. Yu, C. Zhang, A. J. Heeger: Nature **397**, 414 (1999)
53.60 P. Cea, Y. Hua, C. Pearson, C. Wang, M. R. Bryce, M. C. López, M. C. Petty: Mater. Sci. Eng. C **22**, 87 (2002)
53.61 P. Cea, Y. Hua, C. Pearson, C. Wang, M. R. Bryce, F. M. Royo, M. C. Petty: Thin Solid Films **408**, 275 (2002)
53.62 M. Ikai, S. Tokito, Y. Sakamoto, T. Suzuki, Y. Taga: Appl. Phys. Lett. **79**, 156–158 (2001)
53.63 J. Kido, M. Kimura, K. Nagai: Science **267**, 1332 (1995)
53.64 J. Kido, H. Shionoya, K. Nagai: Appl. Phys. Lett. **67**, 2281 (1995)
53.65 J. Thompson, R. I. R. Blyth, M. Mazzeo, M. Anni, G. Gigli, R. Cingolani: Appl. Phys. Lett. **79**, 560 (2001)
53.66 A. R. Duggal, J. J. Shiang, C. M. Heller, D. F. Forest: Appl. Phys. Lett. **80**, 3470 (2002)
53.67 N. S. Saricifti: Mater. Today **7**, 36 (Sept. 2004)
53.68 B. O'Regan, M. Grätzel: Nature **353**, 737 (1991)
53.69 A. Hinsch, J. Kroon, R. Kern, I. Uhlendorf, R. Sastrawan, A. Meyer: Proc. 17th Eur. Photov. Solar Energy Conf. **51**, WIP–Munich and ETA–Florence (2001)
53.70 J. Janata: *Principles of Chemical Sensors* (Plenum, New York 1989)
53.71 J. W. Gardner: *Microsensors* (Wiley, Chichester 1994)
53.72 J. W. Gardner, V. K. Varadan, O. O. Awadelkarim: *Microsensors, MEMS and Smart Devices: Technology, Applications and Devices* (Wiley, Chichester 2001)
53.73 P. T. Moseley, A. J. Crocker: *Sensor Materials* (IOP, Bristol 1996)
53.74 A. S. Snow, W. R. Barger: Phthalocyanine films in chemical sensors. In: *Phthalocyanines: Properties and Applications*, ed. by C. C. Leznoff A. B. P. Lever (VCH, Weinheim 1989) p. 342
53.75 M. C. Petty, R. Casalini: Eng. Science and Education Journal **10**, 99 (2001)
53.76 S. Baker, G. G. Roberts, M. C. Petty: IEE Proc. **130**, 260 (1983)Pt. 1
53.77 S. D. Senturia, C. M. Sechen, J. A. Wishneusky: Appl. Phys. Lett. **30**, 106 (1977)
53.78 P. S. Barker, C. Di Bartolomeo, A. P. Monkman, M. C. Petty, R. Pride: Sensors Actuators B **25**, 451 (1995)
53.79 P. S. Barker, M. C. Petty, A. P. Monkman, J. McMurdo, M. J. Cook, R. Pride: Thin Solid Films **284–285**, 94 (1996)
53.80 J. W. Gardner, P. N. Bartlet: *Electronic Noses: Principles and Applications* (Oxford Univ. Press, Oxford 1999)
53.81 Semiconductor Industry Association Roadmap (2003): http://public.itrs.net/
53.82 J. Greer, A. Korkin, J. Lanbanowski (eds): *Nano and Giga Challenges in Microelectronics* (Elsevier, Amsterdam 2003)
53.83 R. Dettmer: IEE Rev. **49**, 30 (July 2003)
53.84 M. C. Petty: Organic thin-film deposition techniques. In: *Functional Organic and Polymeric Materials*, ed. by T. H. Richardson (Wiley, Chichester 2000) p. 7
53.85 A. Ulman: *Ultrathin Organic Films* (Academic, San Diego 1991)
53.86 M. C. Petty: *Langmuir–Blodgett Films* (Cambridge Univ. Press, Cambridge 1996)

53.87 D. R. Talham: Chem. Rev. **104**, 5479 (2004)
53.88 A. J. Moore, L. M. Goldenberg, M. R. Bryce, M. C. Petty, A. P. Monkman, C. Marenco, J. Yarwood, M. J. Joyce, S. N. Port: Adv. Mater. **10**, 395 (1998)
53.89 L. Netzer, J. Sagiv: J. Am. Chem. Soc. **105**, 674 (1983)
53.90 L. Netzer, R. Iscovici, J. Sagiv: Thin Solid Films **99**, 235 (1983)
53.91 G. Decher, J. D. Hong, J. Schmitt: Thin Solid Films **210/211**, 831 (1992)
53.92 G. Decher, Y. Lvov, J. Schmitt: Thin Solid Films **244**, 772 (1994)
53.93 G. Decher, J. B. Schlenoff (eds): *Multilayer Thin Films* (Wiley-VCH, Weinheim 2003)
53.94 C. Pearson, J. Nagel, M. C. Petty: J. Phys. D: Appl. Phys. **34**, 285 (2001)
53.95 J. H. Cheung, W. B. Stockton, M. F. Rubner: Macromolecules **30**, 2712 (1997)
53.96 Y. Lvov, M. Onda, K. Ariga, T. Kunitake: J. Biomater. Sci. Polym. Edn. **9**, 345 (1998)
53.97 W. B. Stockton, M. F. Rubner: Macromolecules **30**, 2717 (1997)
53.98 S. A. Evanson, J. P. S. Badyal, C. Pearson, M. C. Petty: J. Phys. Chem. **100**, 11672 (1996)
53.99 S. Brittain, K. Paul, X.-M. Zhao, G. Whitesides: Phys. World **11**, 31 (1998)
53.100 R. D. Piner, J. Zhu, F. Xu, S. Hong, C. A. Mirkin: Science **283**, 661 (1999)
53.101 L. F. Chi, L. M. Eng, K. Graf, H. Fuchs: Langmuir **8**, 2255 (1992)
53.102 A. Krämer, R. R. Fuierer, C. B. Gorman: Chem. Rev. **103**, 4367 (2003)
53.103 J. Gimzewski: Phys. World **11**, 25 (1998)
53.104 S. Hong, J. Zhu, C. A. Mirkin: Science **286**, 523 (1999)
53.105 S. Hong, C. A. Mirkin: Science **288**, 1808 (2000)
53.106 X. G. Liu, L. Fu, S. H. Hong, V. P. Dravid, C. A. Mirkin: Adv. Mater. **14**, 231 (2002)
53.107 K. B. Lee, S. J. Park, C. A. Mirkin, J. C. Smith, M. Mrksich: Science **295**, 1702 (2002)
53.108 S. P. Speakman, G. G. Rozenberg, K. J. Clay, W. I. Milne, A. Ille, I. A. Gardner, E. Bresler, J. H. G. Steinke: Organic Electron. **2**, 65 (2001)
53.109 G. PerHin, B. T. Khuri-Yakub: Rev. Sci. Instrum. **73**, 2193 (2002)
53.110 H. Sirringhaus, T. Shimoda (eds): MRS Bull. **28**, 802 (2003)
53.111 I. D. Rees, K. L. Robinson, A. B. Holmes, C. R. Towns, R. O'Dell: MRS Bull. **27**, 451 (2002)
53.112 H. Sirringhaus, T. Kawase, R. H. Friend: MRS Bull. **26**, 539 (2001)
53.113 K. E. Paul, W. S. Wong, S. E. Ready, R. A. Street: Appl. Phys. Lett. **83**, 2070 (2003)
53.114 C. A. Jones, M. C. Petty, G. G. Roberts: IEEE Trans. Ultrasonics Ferroelec. Freq. Control **35**, 736 (1988)
53.115 P. J. Skabara: Organic second-order non-linear optical materials. In: *Functional Organic and Polymeric Materials*, ed. by T. H. Richardson (Wiley, Chichester 2000) p. 295
53.116 A. Aviram, M. A. Ratner: Chem. Phys. Lett. **29**, 277 (1974)
53.117 A. S. Martin, J. R. Sambles, G. J. Ashwell: Phys. Rev. Lett. **70**, 218 (1993)
53.118 G. J. Ashwell, D. S. Gandolfo: J. Mater. Chem. **11**, 246 (2001)
53.119 J. R. Heath, P. J. Kuekes, G. S. Snider, R. S. Williams: Science **280**, 1716 (1998)
53.120 B. G. Streetman, S. Banjeree: *Solid State Electronic Devices* (Prentice Hall, New Jersey 2000)
53.121 R. Compañó (ed): *Technology Roadmap for Nanoelectronics* (Office for Official Publications of the European Communities, Luxembourg 2001)
53.122 S. Kolliopoulou, P. Dimitrakis, P. Normand, H. – L. Zhang, N. Cant, S. D. Evans, S. Paul, C. Pearson, A. Molloy, M. C. Petty: J. Appl. Phys. **94**, 5234 (2003)
53.123 P. E. Burrows, K. J. Donovan, E. G. Wilson: Thin Solid Films **179**, 129 (1989)
53.124 H.-W. Fink, C. Schöneberger: Nature **398**, 407 (1999)
53.125 R. S. Phadke: Appl. Biochem. Biotechnol. **96**, 269 (2001)
53.126 A. Rakitin, P. Aich, C. Papadopoulos, Y. Kobzar, A. S. Vedeneev, J. S. Lee, J. M. Xu: Phys. Rev. Lett. **86**, 3670 (2001)
53.127 C. N. R. Rao, A. K. Cheetham: J. Mater. Chem. **11**, 2887 (2001)
53.128 H. Tabata, L. T. Cai, J. H. Gu, S. Tanaka, Y. Otsuka, Y. Sacho, M. Taniguchi, T. Kawai: Synth. Met. **133–134**, 469 (2003)
53.129 L. Adleman: Science **266**, 1021 (1994)